

# USING DSPACE SYSTEMS FOR TORQUE CONTROL OF ASYNCHRONOUS MOTOR DRIVE

D. FLOROIAN<sup>1</sup> F. MOLDOVEANU<sup>1</sup> L. FLOROIAN<sup>1</sup>

**Abstract:** *We present in this paper a vector control scheme for inverter-fed asynchronous motor, implemented into a dSpace system. The design of the control scheme is carried out considering the model of the motor in a stationary two-phases frame of reference. The rotor flux linkage, the electromagnetic torque and the reactive power are estimated by only using the measure of the three-phases currents and voltages.*

**Key words:** *sliding mode, control systems, real-time systems.*

## 1. Introduction

The asynchronous motor (ASM) is a nonlinear high-order system and for this reason complicated models must be used to control it by using linear control techniques and linear controllers. In addition, due to the complexity of the equations, the signal processing of the control systems is complicated and expensive.

On the other hand the power inverter is also a nonlinear system, because it is composed of power switches (the semiconductors), which are nonlinear elements. The inverter changes the structure of its power circuit depending on which switches are closed or opened. It can be said that an inverter is a nonlinear system with variable structure. Therefore, it is very attractive and logic to use nonlinear control concepts to control inverter-fed ac machines. Several authors recognized this fact publishing very interesting works concerned with sliding mode control of inverter-fed ac machines

[5-9]. In this control method, the structure of the converter is varied depending on the value of logical signals generated by nonlinear controllers [3-7].

This work uses a nonlinear control technique to control an inverter-fed asynchronous motor. The electromagnetic torque and the reactive power are controlled by hysteresis controllers. The outputs of the nonlinear controllers are used in a switching table to generate the command signals. The resulting control scheme is very simple, suitable for high speed implementation. The following pages present the theoretical principles, and the simulation results obtained with this control technique in the field-oriented torque control of an inverter-fed ASM. The mathematical model of the ASM is given in [4].

## 2. Block Diagram of the Control System

The block diagram of a sliding mode control for the electromagnetic and the reactive torque [3], [4] are presented in

---

<sup>1</sup> Centre "Control Process Systems", *Transilvania* University of Braşov.



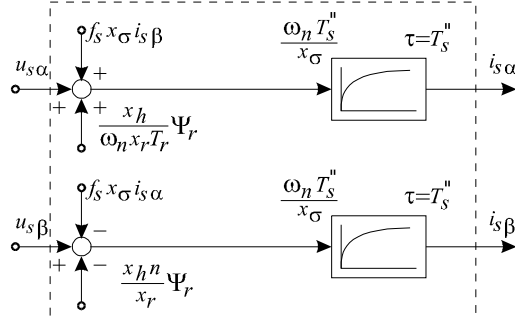


Fig. 2. Block diagram of the ASM

In this work the electromagnetic torque and the reactive torque are controlled separately by using two nonlinear controllers [3]. Figure 3 shows the block diagram of the torque control system.

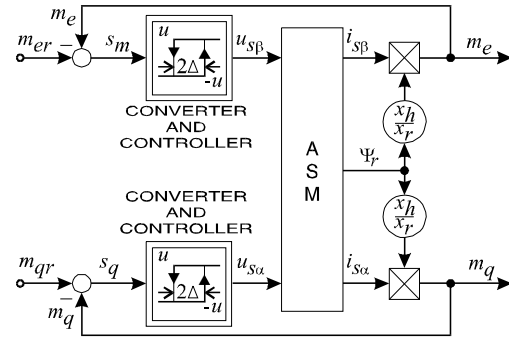


Fig. 3. Control principle of the electromagnetic and reactive torque

The nonlinear elements included in each axis represent the inverter and the nonlinear controllers with hysteresis. The voltage  $u_{s\alpha}$  ( $u_{s\beta}$ ) can take the values  $u$  or  $-u$  depending on the difference between reference and real torques ( $m_{er}$  and  $m_e$  respectively, or  $m_{qr}$  and  $m_q$  respectively). The strategy for the control of the electromagnetic torque is:

$$\begin{aligned} \text{if } s_m > \Delta h_m \text{ then } d_m &= 1 \\ &\text{and } u_{s\beta} = u > 0, \\ \text{if } s_m < \Delta h_m \text{ then } d_m &= 0 \\ &\text{and } u_{s\beta} = -u < 0, \end{aligned} \quad (4)$$

and for the control of the reactive torque is:

$$\begin{aligned} \text{if } s_q > \Delta h_q \text{ then } d_q &= 1 \\ &\text{and } u_{s\alpha} = u > 0, \\ \text{if } s_q < \Delta h_q \text{ then } d_q &= 0 \\ &\text{and } u_{s\alpha} = -u < 0, \end{aligned} \quad (5)$$

where  $d_m$  and  $d_q$  are output variables of the nonlinear controllers. In compact form, we have:

$$d_q = \Gamma(u_{s\alpha}), \quad (6)$$

$$d_m = \Gamma(u_{s\beta}), \quad (7)$$

where:

$$\Gamma(x) = \begin{cases} 0 & \text{if } x < 0, \\ 1 & \text{if } x > 0. \end{cases} \quad (8)$$

The control strategy uses the voltages  $u_{s\alpha}$  and  $u_{s\beta}$  but the converter applies the voltages  $u_{10}$ ,  $u_{20}$  and  $u_{30}$  to the phases of the motor. For this reason, the next step is to find the relation between the voltages  $u_{10}$ ,  $u_{20}$ ,  $u_{30}$  and  $u_{s\alpha}$ ,  $u_{s\beta}$ .

In [1] it was demonstrated that this inverter applies eight voltage space vectors to the motor.

Each vector corresponds to one configuration of the branch command signals  $d_1$ ,  $d_2$ ,  $d_3$  as illustrated in Table 1.

 Table 1  
Generation of the voltage space vectors

Voltage Space Vector	$d_1$	$d_2$	$d_3$
$\underline{u}_{s1}^s$	1	0	0
$\underline{u}_{s2}^s$	1	1	0
$\underline{u}_{s3}^s$	0	1	0
$\underline{u}_{s4}^s$	0	1	1
$\underline{u}_{s5}^s$	0	0	1
$\underline{u}_{s6}^s$	1	0	1
$\underline{0}$	0	0	0
$\underline{0}$	1	1	1

The complex plane of Figure 4 is divided into six sectors. Each sector is limited by two voltage space vectors, as illustrated in Figure 4. This figure includes also the rotating ( $\alpha, \beta$ ) frame of reference. The components of each space vector in the  $\alpha$  and  $\beta$ -axis are the voltages  $u_{s\alpha}$  and  $u_{s\beta}$  respectively.

For the torque (current) control it is important to detect the position of the frame of reference ( $\alpha, \beta$ ) in order to select adequately the voltage space vector [3], [5]. In this work, the  $\alpha$ -axis is oriented with the rotor flux of the motor to implement a field-oriented control. Table 2 shows the commutation logic of the three-phase inverter, for different positions of the  $\alpha$ -axis.

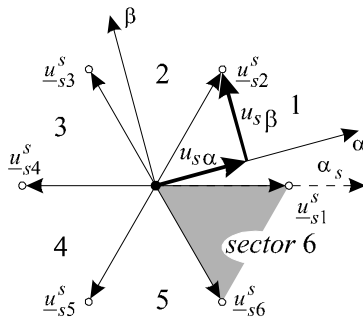


Fig. 4. The sectors of the complex plane

Table 2

Commutation logic of the three-phase inverter

Sector	0	0	1	1	$d_m$
	0	1	0	1	$d_q$
1	5	1	4	2	
2	6	2	5	3	
3	1	3	6	4	
4	2	4	1	5	
5	3	5	2	6	
6	4	6	3	1	

To understand this table, the different variables are now analyzed, when the  $\alpha$ -axis is located in sector 1.

If the output of the current controllers are  $d_m = 0$  and  $d_q = 0$ , this means that the

voltages  $u_{s\alpha}$  and  $u_{s\beta}$  must be negative to reduce the currents  $i_{s\alpha}$  and  $i_{s\beta}$ . In this case the space vector  $\underline{u}_{s1}^s$  must be applied to the motor, because this space vector has two negative components:  $u_{s\alpha} < 0$  and  $u_{s\beta} < 0$ .

If the outputs of the current controllers are  $d_m = 0$  and  $d_q = 1$ , this means that current  $i_{s\alpha}$  must increase and current  $i_{s\beta}$  must decrease, which is accomplished by applying the voltages  $u_{s\alpha} > 0$  and  $u_{s\beta} < 0$  to the stator. In this second case, the space vector  $\underline{u}_{s1}^s$  is applied to the motor.

The space vector  $\underline{u}_{s6}^s$  is here discarded, because it has a too small component  $u_{s\alpha}$ . If  $d_m = 1$  and  $d_q = 1$ , the voltages  $u_{s\alpha}$  and  $u_{s\beta}$  must be positive to produce an increase in the currents  $i_{s\alpha}$  and  $i_{s\beta}$ . This is accomplished with space vector  $\underline{u}_{s1}^s$ . Finally, if  $d_m = 1$  and  $d_q = 0$ , current  $i_{s\alpha}$  must decrease and current  $i_{s\beta}$  must increase. In this situation space vector  $\underline{u}_{s4}^s$  is applied to the load, because it has  $u_{s\alpha} < 0$  and  $u_{s\beta} > 0$ . This analysis is repeated in each sector. As for the control strategy it is sufficient to know in which of sectors 1...6 stator angle  $\theta_s$  is positioned; this can be computed by the signs of three linear combinations of the estimated rotor flux components:

$$s_1 = \text{sign}(\Psi_{r\alpha}^s), \tag{9}$$

$$s_2 = \text{sign}(\Psi_{r\alpha}^s - \sqrt{3}\Psi_{r\beta}^s), \tag{10}$$

$$s_3 = \text{sign}(\Psi_{r\alpha}^s + \sqrt{3}\Psi_{r\beta}^s). \tag{11}$$

Table 3

Establishing the sector of  $\theta_s$  with respect to the three signs  $s_1, s_2$  and  $s_3$

$s_1$	1	1	-1	-1	-1	1
$s_2$	1	-1	-1	-1	1	1
$s_3$	1	1	1	-1	-1	-1
Sector	1	2	3	4	5	6

Table 3 gives the sector of stator angle  $\theta_s$  with respect to the three signs  $s_1, s_2$  and  $s_3$ .

#### 4. dSpace Experimental Results

In order to analyze the performance of the proposed system, a numerical simulation has been utilized. All data processing for the simulations have been carried out in p.u. form. The induction machine considered in the simulation is a three phase, squirrel cage machine.

When the system is in the steady-state of the real sliding mode, the switching law must evolve inside the switching domain. If the switching device consists of two Schmitt triggers, the switching domain will be a rectangle comprised between the „thresholds” of the hysteresis zones (the switching lines) of the two comparators.

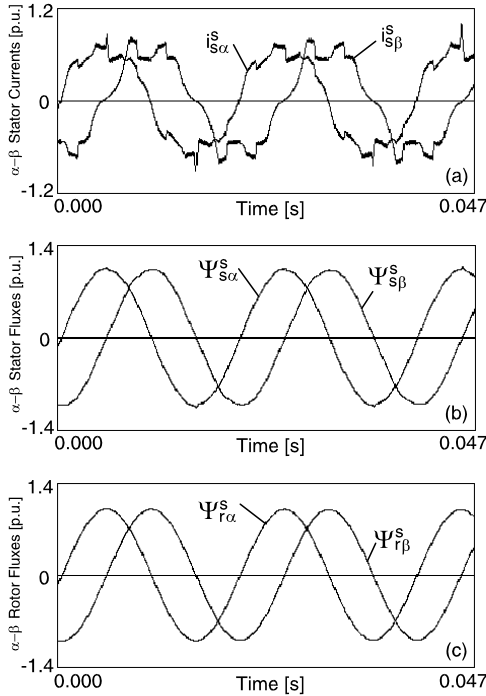


Fig. 5. Steady-state wave shapes of the stator currents (a), stator fluxes (b), and rotor fluxes (c)

Also, in steady-state, the complex torque:

$$\underline{m} = m_q + jm_e = \frac{x_h}{x_r} \Psi_r \dot{i}_s, \quad (12)$$

evolves within the switching domain and the phase quantities are sinusoidal with overlapping ripple, due to the real sliding mode. Figure 5 shows the wave shapes of the stator currents, stator and rotor fluxes, for the following numerical values:

$$\begin{aligned} \Delta h_m &= 0.10 \text{ p.u.}, m_{er} = 0.800 \text{ p.u.}, \\ \Delta h_q &= 0.20 \text{ p.u.}, m_{qr} = 0.517 \text{ p.u.} \\ n &= 0.5 \text{ p.u.} \end{aligned} \quad (13)$$

Figure 6 presents the wave shapes of the electromagnetic and reactive torques in the steady-state. For the same example, Figure 7 shows the space phasors of the stator current, stator and rotor flux represented by phasors diagrams. The ripple of the complex torque is visible on the stator current phasor diagram, while the space phasors of the stator and rotor flux evolve on a circular trajectory.

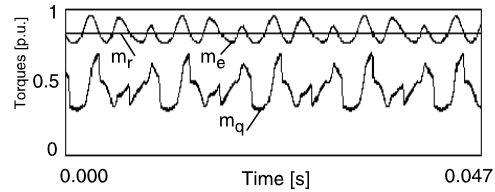


Fig. 6. Steady-state wave shapes of the electromagnetic and reactive torques

#### 5. Conclusions

A control scheme for inverter-fed asynchronous motor has been presented. A simple model of the induction machine suited for nonlinear control has been presented. The model has two time constants and several terms, which are considered as perturbations in the control. Two nonlinear controllers are used to control the electromagnetic torque and the reactive power in a rotating frame of

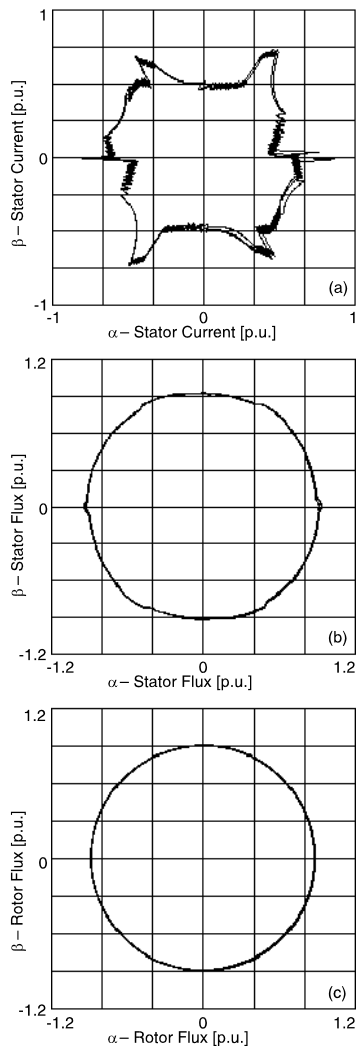


Fig. 7. Diagrams of steady-state stator current (a), stator flux (b), and rotor flux (c) space phasors

reference. The controllers are very robust, because they are not affected by strong perturbations. The output signals of the nonlinear controllers are used in a switching table to generate the command signals of the three-phases inverter.

Space vectors were used to establish the relation between voltages  $u_{s\alpha}$ ,  $u_{s\beta}$  and the terminal voltages of the stator  $u_{10}$ ,  $u_{20}$  and  $u_{30}$ . This work shows that the use of space vectors is a very effective method to analyze the work of a voltage source inverter.

Finally, it can be said that the drive has a very good dynamic behavior with simple operation, few circuits and reduced costs.

## References

1. Doan, P.T., Nguyen, T.T., et al.: *Sensorless Vector Control of AC Induction Motor Using Sliding-Mode Observer*. In: *Int. J. Science and Engineering* **4** (2013) No. 2, p. 39-43.
2. Lascu, C., Boldea, I., Blaabjerg, F.: *Direct Torque Control of Sensorless Induction Motor Drives: A Sliding-Mode Approach*. In: *IEEE Trans. on Industry Applications* **40** (2004) No. 2, p. 582-590.
3. Lascu, C., Trzynadlowski, A.M.: *Combining the Principles of Sliding Mode, Direct Torque Control, and Space-Vector Modulation in a High-Performance Sensorless AC Drive*. In: *IEEE Trans. on Industry Applications* **40** (2004) No. 1, p. 170-177.
4. Patrel, B.M., Panchade, V.M., Nagarale, R.M.: *Sliding Mode Control of DC Drives*. In: *Sliding Mode Control*, (Ed. A. Bartoszewicz), InTech, April 2011, p. 167-180.
5. Šabanović, A., Šabanović-Behlilović, N.: *Sliding Modes in Electrical Drives and Motion Control*. In: *The 18<sup>th</sup> IFAC World Congress, Milano, 2011*, p. 756-761.
6. Sabanovic, A., Fridman, L., Spurgeon, S.: *Variable Structure Systems: from Principles to Implementation*. In: *The Institution of Electrical Engineers*, 2004.
7. Utkin, V.I.: *Sliding Modes in Control Optimization*. Springer-Verlag, 2010.
8. Utkin, V.I., Guldner, J., Shi, J.: *Sliding Mode Control in Electromechanical Systems*. Taylor & Francis, 2009.
9. Zhou, Y., Wang, B.L.: *PWM-Quasi-Sliding Mode Control for APFC Converters*. In: *Electrical Engineering* **92** (2010) No. 2, p. 43-48.